

Optimal control of wheel loader operation in the short loading cycle using two braking alternatives

Vaheed Nezhadali and Lars Eriksson
Electrical Engineering Department
Vehicular systems division
Linköping University, Sweden
Email: {vahne23, larer}@isy.liu.se

Abstract—The optimal control of wheel loader operation is used in order to investigate the potentials for fuel cost and cycle time minimization during the short loading cycle. The wheel loader is modeled as a nonlinear system with three control inputs and four state variables where a diesel engine generates the power utilized for lifting and traction. The lifting system is modeled considering the limitations in the hydraulics and also the structural constraints. A torque converter is included in the driveline model which introduces nonlinearities into the system and operates in different modes affecting the fuel consumption. The gear shifts during the loading cycle impose a discrete variable into the system and this is taken care of by representing the loading cycle as a multi-phase optimal control problem with constant gearbox gear ratio in each phase. Minimum fuel and minimum time system transients are calculated and analyzed for two alternative cases one where the torque converter is used to stop the vehicle before reaching the reversing point and another where the service brakes are utilized. The optimal control problem is iteratively solved in order to obtain the trade-off between fuel consumption and cycle time for both braking alternatives. It is shown that although the engine operates at lower speeds when the torque converter is used for braking, the fuel consumption increases as higher torques are demanded from the engine during braking. The increase in fuel consumption is higher in faster cycle operations as the vehicle travels at higher speeds and larger torques are required to stop the vehicle. Wheel loader operators tend to use torque converter braking alternative as it is more convenient; however, it accompanies higher fuel consumption which highlights the importance of developing intelligent and easy to use braking systems.

I. INTRODUCTION

The short loading cycle is a frequent application of wheel loaders which is a combination of load lifting and transportation, Fig 1. The minimization of fuel consumption and cycle time is interesting for the manufacturers as it would increase the productivity and reduce the costs in construction projects. However, these objectives are contradictory and a desirable compromise between the two can be obtained by the optimal control study of wheel loader operation instead of performing costly experimental measurements. The knowledge gained by optimal control is also helpful in the design process of control algorithms for autonomous wheel loader control systems, [1].

In [2] a model was developed for the wheel loader including a torque converter (TC) capable of transferring power from the engine to the wheels and vice versa. The power distribution in the system was analyzed and it was concluded that the TC is

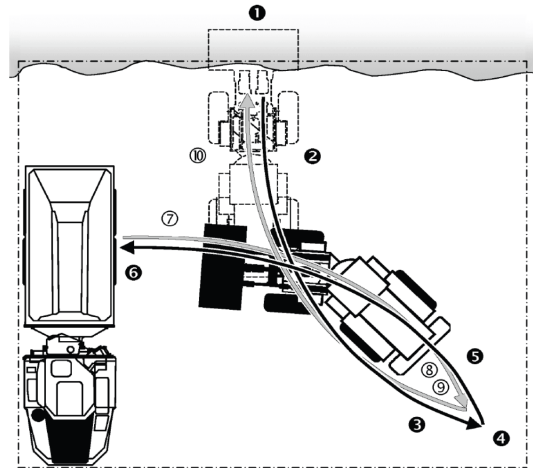


Fig. 1. Numbered sequence of actions in a short loading cycle, point 4 is called the reversing point, picture from [5].

the key component in the driveline as it introduces the largest power losses into the system.

Using the TC for braking, called TC braking in this paper, is done by shifting into forward gear before the reversing point, around point 3 on Fig 1, and is found easier by the drivers since the gas pedal is used even for braking. The contribution of this paper is the optimal control study of the alternative braking technique where either service brakes or TC is utilized in order to reduce the vehicle speed.

The wheel loader components are modeled according to the properties in [3]. PROPT [4] which uses pseudo-spectral collocation methods is used to solve the formulated multi-phase optimal control problem and all constants and parameters used in the modeling section are exactly the same as in [2].

II. SYSTEM MODEL

Fig 2 shows the components in the wheel loader model and the interdependence between them. The consists of models for diesel engine, lifting system, TC, gearbox and vehicle longitudinal dynamics. The states are engine speed ω_{ice} , vehicle speed V , bucket height H_{buc} , and bucket speed V_{buc} while the control inputs are fuel injection per engine cycle U_{mf} , bucket vertical acceleration U_{ab} , and braking signal at wheels U_b . The governing differential equations of the system, used to determine the states are:

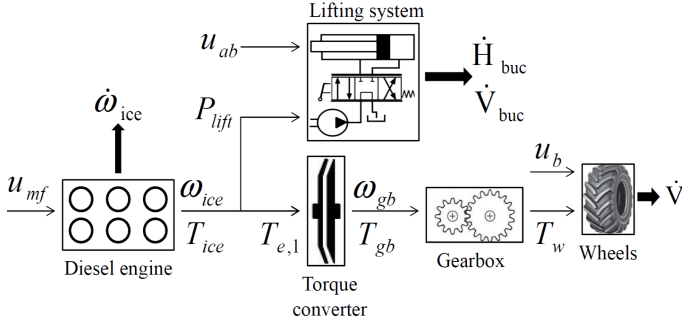


Fig. 2. Wheel loader system model showing the interdependence between system components.

$$\frac{d\omega_{ice}}{dt} = \frac{1}{J_{ice}} \left(T_{ice}(U_{mf}, \omega_{ice}) - \frac{P_{load}(V_{buc}, V)}{\omega_{ice}} \right) \quad (1)$$

$$\frac{dV}{dt} = \frac{sign(V) (F_{trac}(U_b, \omega_{ice}) - F_{roll})}{M_{tot}} \quad (2)$$

$$\frac{dH_{buc}}{dt} = V_{buc} \quad (3)$$

$$\frac{dV_{buc}}{dt} = U_{ab} \quad (4)$$

where γ is the gearbox gear ratio and the power request from the diesel engine P_{load} is calculated as the sum of the powers required for lifting P_{lift} and vehicle traction P_{trac} . The $sign$ function in the model equations has a constant value during each phase of the operation and does not cause discontinuities.

A. Diesel engine

A simplified version of the mean value engine model developed in [6] is used as the power source in the system. The engine torque T_{ice} is calculated based on the friction torque T_{fric} and indicated gross torque T_{ig} . The torques and the mass of injected fuel during each combustion cycle \dot{m}_f are calculated as follows:

$$T_{ice}(U_{mf}, \omega_{ice}) = T_{ig}(U_{mf}) - T_{fric}(\omega_{ice}) \quad (5)$$

$$T_{ig}(U_{mf}) = \frac{\eta_{ig} q_{hv} n_{cyl} U_{mf} 10^{-6}}{4\pi} \quad (6)$$

$$T_{fric}(\omega_{ice}) = \frac{V_d 10^5}{4\pi} (c_{fr1} \omega_{ice}^2 + c_{fr2} \omega_{ice} + c_{fr3}) \quad (7)$$

$$\dot{m}_f(U_{mf}, \omega_{ice}) = \frac{10^{-6}}{4\pi} U_{mf} \omega_{ice} n_{cyl} \quad (8)$$

where η_{ig} and $c_{fr1,2,3}$ are the tuning parameters of the model, q_{hv} is the heating value of the fuel, n_{cyl} is the number of cylinders and V_d is the total cylinder displacement volume.

B. Lifting system

The power required for lifting P_{lift} and system constraints during the lifting are calculated in the lifting system model. It is assumed that no power is required for holding the loaded bucket at a constant height. The lifting power is calculated as:

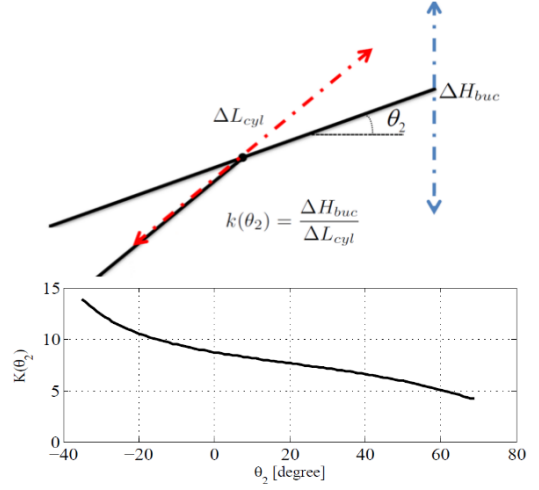


Fig. 3. The vertical displacement of the bucket is equal to the multiplication of the lift cylinder displacement into variable $k(\theta_2)$.

$$F_{load} = M_{load} (g + U_{ab}) \quad (9)$$

$$P_{lift,net} = F_{load} V_{buc} \quad , \quad P_{lift} = \frac{P_{lift,net}}{\eta_{lift}} \quad (10)$$

where g is the earth gravity, η_{lift} is the efficiency of the lifting system and M_{load} is the sum of bucket mass and the maximum capacity of the bucket. During the lifting, the vertical displacement of the end point of the boom is calculated as the multiplication of the lift piston displacement ΔL_{cyl} with a non-constant factor k which depends on the height of the bucket, see Fig 3 and Fig 4 for the nomenclature in the following equations. The values of k at different boom angles θ_2 are calculated as follows:

$$\theta_2 = \sin^{-1} \left(\frac{H_{buc} - G}{r} \right), \quad \theta_1 = \tan^{-1} \left(\frac{r_1 \cos(\theta_2) - x_c}{r_1 \sin(\theta_2) - y_c} \right) \quad (11)$$

$$L_{cyl} = \sqrt{(r_1 \cos(\theta_2) - x_c)^2 + (r_1 \sin(\theta_2) - y_c)^2} \quad (12)$$

$$k(\theta_2) = \frac{\Delta(r \sin(\theta_2)) / \Delta\theta_2}{\Delta L_{cyl} / \Delta\theta_2} \quad , \quad r = r_1 + r_2 \quad (13)$$

where G is the height of the joint between boom and the wheel loader body. The lifting is performed by hydraulic lift cylinders and it should be ensured that the exerted pressure on the lift cylinders does not exceed the component limit. Considering the boom as a beam with the moment of inertia of I_{boom} , the exerted force on the lift cylinders, F_p , is calculated by solving the moment equilibrium equation around where the boom is connected to the wheel loader body.

$$F_p = \frac{\frac{I_{boom} U_{ab}}{r} + F_{load} r \cos(\theta_2) + F_w \frac{r}{2} \cos(\theta_2)}{r_1 \sin(\theta_1 - \theta_2)} \quad (14)$$

$$F_w = M_{boom} (g + U_{ab}) \quad (15)$$

where M_{boom} is the mass of the boom. knowing the piston surface area of the lift cylinder A_{piston} the exerted pressure in the lift cylinder is calculated as follows:

$$P_{cyl} = \frac{F_p}{A_{piston}} \quad (16)$$

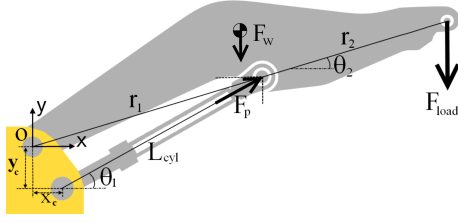


Fig. 4. The boom, lift cylinder and acting forces on the boom.

The amount of fluid delivered to the lift cylinders by the hydraulic pump defines the displacement speed of the lift cylinder and its maximum can be calculated using the maximum pump displacement $D_{pump,max}$ and the dimensions of the hydraulic cylinder (r_{piston} and r_{rod}) available in [3]. Hydraulic pump speed is same as the engine speed until it saturates at around 1500 rpm. The maximum possible piston displacement speed in the lift cylinder $v_{pist,max}$ is then calculated as follows:

$$A_{piston} = \pi (r_{piston}^2 - r_{rod}^2) \quad (17)$$

$$Q_{pump} = \min(\omega_{ice}, 1500) \times D_{pump,max} \eta_{volumetric} \quad (18)$$

$$v_{pist,max} = \frac{Q_{pump} \eta_{cyl,l}}{A_{piston}} \quad (19)$$

where $\eta_{volumetric}$ and $\eta_{cyl,l}$ are constant, and describe the volumetric efficiency of the hydraulic pumps and the mechanical efficiency of the lift cylinders. The upper limit on the lifting speed $V_{lift,max}$ is then calculated as:

$$V_{lift,max} = k(\theta_2) v_{pist,max} \quad (20)$$

C. Torque converter and gearbox model

TC dynamics can be studied when the model is expressed in terms of differential equations [7]. A static nonlinear model suitable for control studies represents the TC here, as in [8]. The TC is modeled based on characteristics curves, and the technique described in [2] is used to avoid the discontinuities in the model. The pumping side of the TC rotates at the speed of the diesel engine and the turbine side is directly connected to the gearbox, see Fig 2. The speed ratio ϕ over the TC and the gearbox speed ω_{gb} are calculated as:

$$\phi = \frac{\omega_{gb}}{\omega_{ice}}, \quad \omega_{gb} = \frac{V \gamma}{r_w} \quad (21)$$

where r_w is the wheel radius. The generated torque in the pumping side of the TC T_p , and the transferred torque to the gearbox side T_{gb} are calculated as:

$$T_p = \xi(\phi) \left(\frac{\omega_{ice}}{1000} \right)^2, \quad T_{gb} = \kappa(\phi) \left(\frac{\omega_{ice}}{1000} \right)^2 \quad (22)$$

where $\kappa(\phi)$ and $\xi(\phi)$ are the TC characteristic curves illustrated in Fig 5. Including a constant gearbox efficiency η_{gb} the delivered torque to the wheels T_w can be calculated as follows:

$$T_w = T_{gb} \eta_{gb} \gamma \quad (23)$$

TABLE I
TC OPERATING MODE DEPENDS ON THE ϕ VALUE

Mode	Speed ratio (ϕ)
I	$\phi < 0$
II	$0 \leq \phi \leq 1$
III	$1 < \phi$

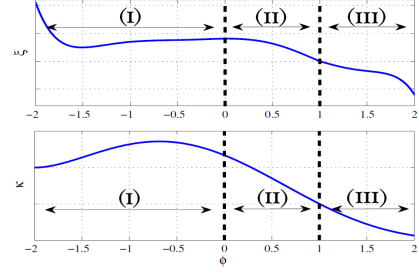


Fig. 5. Torque converter characteristic curves and different operating ranges.

Depending on the ϕ value, the TC can operate in three different operating modes described in table I. The TC operates in mode II when the power is transferred from the engine side to the gearbox side during vehicle acceleration. While the wheel loader travels backwards if forward gear is selected ($\gamma = 60$ and $V < 0$) the two sides of the TC will rotate in opposite directions ($\phi < 0$) and the torque transferred through the TC would reduce the vehicle speed, mode I. Mode III happens when the engine speed becomes lower than the gearbox speed ($\phi > 1$). In this mode the kinetic energy of the wheels is transferred to the engine side of the TC and decreases the deceleration rate of the engine.

The demanded power in the driveline during modes I and II and the transmitted power during mode III is calculated as:

$$P_{trac} = T_p \omega_{ice} \quad (24)$$

D. longitudinal dynamics

The vehicle acceleration is calculated by solving the vehicle longitudinal dynamics. Aerodynamic resistive forces are neglected due to low vehicle velocities and only the rolling resistance F_{roll} is taken into account. Total mass of the vehicle M_{tot} is calculated as the sum of the vehicle mass M_{veh} , the equivalent mass of rotating wheels and M_{load} . The vehicle acceleration is calculated as:

$$F_{roll} = c_r (M_{veh} + M_{buc}) g \quad (25)$$

$$F_{trac} = \frac{T_w - \text{sign}(V) T_b}{r_w}, \quad T_b = U_b \quad (26)$$

$$M_{tot} = M_{veh} + M_{buc} + \frac{4 J_w}{r_w^2} \quad (27)$$

$$\frac{dV}{dt} = \frac{\text{sign}(V) (F_{trac} - F_{roll})}{M_{tot}} \quad (28)$$

where J_w is the wheel inertia and c_r is the rolling resistance coefficient.

III. PROBLEM FORMULATION

The fuel consumption in the lift-transport section of the short loading cycle and the time of this operation is calculated

TABLE II
THE STRUCTURE OF MULTI-PHASE OPTIMAL CONTROL PROBLEM FORMULATION WHERE $\gamma = 0/60$ IN THE THIRD COLUMN REPRESENTS THE TWO ALTERNATIVES FOR BRAKING.

	Phase 1 Reversing $\gamma = -60$ $U_b = 0$	Phase 2 Reversing $\gamma = 0$ or $= 60$ $U_b \neq 0$ or $= 0$	Phase 3 Forwarding $\gamma = 60$ $U_b = 0$	Phase 4 Forwarding $\gamma = 0$ $U_b \neq 0$
t	0	t_1	t_1 t_2	t_2 t_3 t_3 T
ω_{ice}	1500 [rpm]	-	-	-
V	0	-	0	0
V_{buc}	0	-	-	0
H_{buc}	0.7 [m]	-	-	5 [m]
\dot{x}	-	-	-	0

for two alternative braking methods. First, using service brakes represented by the braking control input U_b , and second using the TC braking. An optimal control problem is solved to find the optimal system transients and since the gearbox gear ratio changes discontinuously during the the lift-transport operation a multi-phase optimal control problem where γ remains constant during each phase is formulated. Different phases and boundary conditions of the multi-phase optimal control problem are presented in table II. At $t = 0$ the vehicle has finished the bucket filling process and the engine speed is not at its minimum. The loaded bucket should be lifted up to 5 meters at the end of the operation and the traveling distance in the reversing and forwarding sections of the cycle are the typical value in the short loading cycles equal to 1.5 times the circumference of a wheel which becomes 6.6 meters. The wheel loader fuel consumption in the lift-transport section of the short loading cycle is then calculated by:

$$M_f = \int_0^{t_1} \dot{m}_f dt + \int_{t_1}^{t_2} \dot{m}_f dt + \int_{t_2}^{t_3} \dot{m}_f dt + \int_{t_3}^T \dot{m}_f dt \quad (29)$$

where \dot{m}_f in each phase is calculated by (8). The system transients and gear shifting times (t_1 , t_2 and t_3) in the minimum fuel and minimum time operation are calculated by solving the following optimal control problems:

$$\begin{aligned} \min M_f \quad \text{or} \quad \min T \\ \text{s.t: } \dot{x} = f(x, u) \end{aligned} \quad (30)$$

where \dot{x} are determined by (1) - (4) and the system constraints are:

$$\begin{aligned} \int_0^{t_2} V dt = -6.6 \quad \int_{t_2}^T V dt = 6.6 \\ T_{ice} \leq T_{ice,max}(\omega_{ice}) \quad V_{buc} \leq V_{lift,max} \\ \omega_{ice,min} \leq \omega_{ice} \leq \omega_{ice,max} \quad P_{cyl} \leq P_{cyl,max} \\ -0.18 g \leq \frac{dV}{dt} \quad |V| \leq V_{max} \end{aligned} \quad (31)$$

The $T_{ice,max}(\omega_{ice})$ constraint is modeled as three linear upper bounds on the engine torque as illustrated in Fig 7. The constraint on the derivative of vehicle speed is applied to ensure the stability of the wheel loader during braking since the loaded bucket is raised and fast decelerations could cause damages to the mechanical structure. In addition to the above

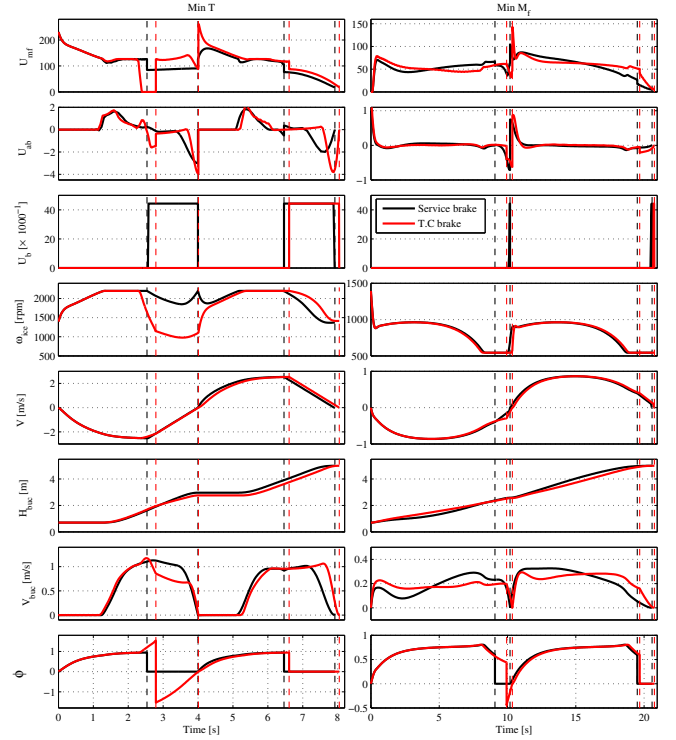


Fig. 6. Time and fuel optimal control and state trajectories for both braking alternatives, vertical dashed lines are phase boundaries.

constraints, the states must be continuous between the successive phases and this is ensured by applying the following phase connecting constraints in PROPT:

$$\begin{aligned} x_i \text{ at the start of phase } j+1 = x_i \text{ at the end of phase } j \quad (32) \\ i \in \{1, 2, 3, 4\} \text{ and } j \in \{1, 2, 3\} \end{aligned}$$

Using PROPT to solve the formulated optimal control problem in (30) with respect to the constraints in (31) and (32) results in oscillatory controls and states. To remove the oscillations, a penalty on the derivatives of the oscillatory control inputs, as formulated in (33), is added to the criterion function in (30), and the problem is solved iteratively by decreasing the penalty coefficient k until $k = 0$. This removes the oscillations while the system dynamics remain almost unchanged. Using this technique, the largest change in the objective function value is only 0.3 %.

$$k \left(\int_0^T \dot{U}_{ab}^2 dt + \int_0^T \dot{U}_{mf}^2 dt \right) \quad , \quad k \rightarrow 0 \quad (33)$$

IV. RESULTS

A. Optimal system transients

The left and right columns in Fig 6 show the optimal controls and system transients for both of the braking alternatives in time and fuel optimal cycles respectively. The last plot in the same figure shows the ϕ value during the wheel loader operation which is helpful to verify the TC operating mode. Fig 7 shows the engine operating points on the engine map with respect to the engine torque limit.

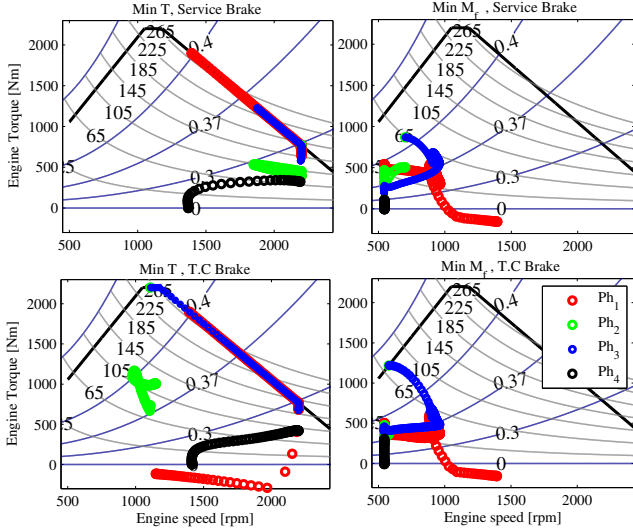


Fig. 7. Engine operating points in time and fuel optimal transients with respect to the engine torque limits for both braking alternatives (constant efficiency curves in blue and constant power [kW] curves in gray).

The time optimal transients, in both braking alternatives, start by delivering all diesel engine power to the driveline for fastest possible acceleration. Then the load lifting starts when the vehicle has already reached high speeds and the most of the engine power can be delivered to the lifting system. The limit on the maximum lift cylinder pressure becomes active only in short periods of the time optimal transients and the effect is seen as the lowered rate of increase in U_{ab} between 1.1 and 1.4 seconds. At the end of the first phase in the TC braking alternative, the fuel injection is cut off and the engine speed drops quickly. In this interval, $\phi > 1$ and the TC operates in mode III providing excess power for lifting which is the reason for the sudden increase in U_{ab} moments before entering the second phase.

When the TC is used for braking, the engine power is used for both braking and lifting during the second phase. In order to consume less power for the braking and leave more power for the lifting, starting from the end of the first phase, the engine is controlled towards speeds where according to Fig 5, ξ has lowest values in the $\phi < 0$ region which results in lower power request at wheels during braking according to (24). The braking continues with maximum possible deceleration until the end of the second phase.

When service brakes are used, no power is demanded by the driveline during the second phase and the engine speed remains high enough only to continue the lifting process at almost constant lifting speed until moments before reversing point where the bucket is decelerated to zero speed. The third phase in both braking alternatives starts in the same way as the first phase and since $V_{buc} = 0$ the whole engine power is allocated for vehicle acceleration. In case of using service brakes, the third phase starts by a slight decrease in the engine speed and increase in the fuel injection level to produce larger engine powers, see the blue points in the top-left plot in Fig 7, useful for faster accelerations and then continues on the engine

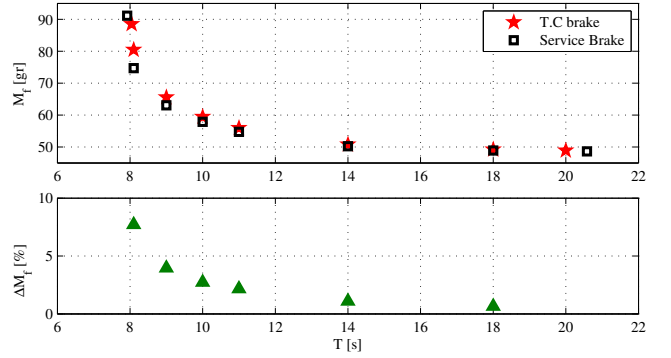


Fig. 8. Trade-off between cycle time and fuel consumption (top). Increase in fuel consumption when TC braking is used (bottom).

speed limit as in the first phase.

In both braking alternatives, by shifting into neutral gear in the fourth phase the driveline is decoupled from the engine and the engine power is used only for lifting while the brakes are used to stop the vehicle as fast as permitted by the deceleration limit. The final bucket deceleration happens later in the cycle in case of the TC braking alternative in order to compensate for the lower lifting speeds during the second phase. When the service brakes are used, the TC never operates in mode III since there is no drastic drop in the engine speed level while the gearbox is engaged.

In the fuel optimal transients, the system is controlled into low engine speeds in order to minimize the power losses as discussed in [2]. In both braking alternatives the lifting and vehicle acceleration are performed simultaneously during the cycle. In the first and third phases, the vehicle starts from stand still and lifting speed is zero but U_{mf} is smaller at the beginning of the first phase since less fuel is required as the kinetic energy of the engine is used for acceleration and lifting by a rapid deceleration in the engine speed which is higher at the beginning of the first phase. In both braking alternatives, the TC operates always in mode II unless the second phase where TC is used for braking (mode III) or when the gearbox is in neutral (phase four).

B. Trade-off between minimum fuel and minimum time transients

The optimal control problem in (30) is reformulated as the weighted sum of the fuel and time objectives:

$$\min (W_1 M_f + W_2 T) + k \left(\int_0^T U_{ab}^2 + \int_0^T U_{mf}^2 \right) \quad (34)$$

$$\text{s.t. } \dot{x} = f(x, u) \ \& \ W_1 + W_2 = 1$$

The penalizing technique with $k \rightarrow 0$ is applied to obtain smooth system transients. The formulated problem is solved for different values of W_1 and W_2 starting from $W_2 = 0$. The results show that using the TC braking alternative slightly affects the cycle duration and increases the cycle time by 1.58 % and 2.8 % in the time optimal and fuel optimal transients respectively. In Fig 8 the trade-off between fuel consumption and cycle time using the two braking alternatives

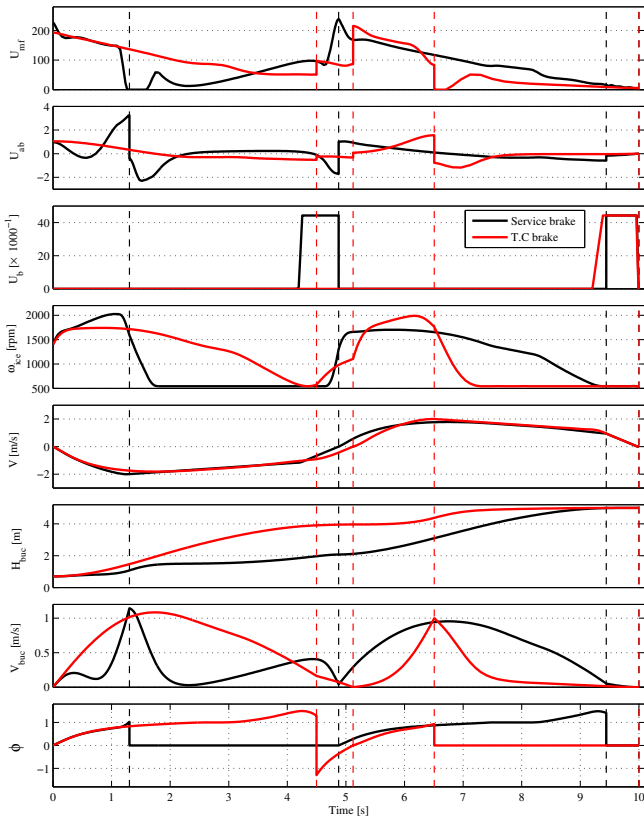


Fig. 9. Fuel optimal control and state trajectories in 10 sec cycle for both braking alternatives, vertical dashed lines are phase boundaries.

is illustrated. The Pareto front shows that reducing the fuel optimal cycle length by 50 % would cause less than 10 % increase in the fuel consumption and fuel consumption would decrease up to 35 % if the time optimal cycle duration is increased by only 10 %. The lower plot in the same figure shows the percentage of increase in the fuel consumption when the TC braking is used instead of service brakes (the difference is calculated at points where the cycle times are identical). In faster cycles the wheel loader speed is higher and larger engine torques are required to stop the vehicle time optimally resulting in larger fuel consumptions in case of TC braking.

The Pareto shows a satisfying compromise between the fuel and time criteria in the 9 to 11 second cycles. Fig 9 shows the system transients for both braking alternatives where the controls minimize the fuel consumption in a 10 sec cycle. In both braking alternatives, the load is mostly lifted only in one half of the cycle in which the engine speed remains relatively high, and in the other half of the cycle, the engine speed decreases to the minimum limit right after the vehicle has reached high velocities. The fuel consumption is 2.7 % higher in TC braking alternative as more power is generated by the engine during the cycle operation, and in both braking alternatives, the TC operates in modes II and III when the vehicle accelerates.

V. CONCLUSION

A wheel loader model with four states and three control inputs including a torque converter model is used to study

minimum time and minimum fuel system transients. The torque converter is modeled so that it can be used to stop the vehicle during reversing without using the service brakes. The gearbox gear ratio varies discretely during the lift-transport section of the short loading cycle. To avoid the difficulties of solving mixed integer optimal control problems, a multi-phase optimal control problem, with constant gearbox gear ratio during each phase, is formulated and solved. The results show that, in the time optimal transients, the direction of power transfer in the torque converter is mostly towards the wheels, unless, the torque converter is used to stop the vehicle by shifting into forward gear before the reversing point where the transferred torque reduces the vehicle speed. In both reversing and forwarding sections of the time optimal loading cycle, the power is first allocated to the vehicle acceleration whereas load lifting starts when the vehicle has reached high velocities. However, in the fuel optimal case, the lifting and vehicle acceleration are performed simultaneously during the forwarding and reversing sections, while the engine operates at lower speeds in order to minimize the power losses and fuel consumption. The fuel consumption is calculated for eight different cycle durations and the trade-off between the fuel and time criteria is presented as a Pareto front. When the torque converter is used for braking, the fuel consumption increases at all cycle durations. The increase in the fuel consumption is higher at faster cycles as more engine power is required to stop the wheel loader traveling at higher velocities. Although using the torque converter during braking is easier for the drivers, it is shown that it increases the fuel consumption. Therefore, it is important to use intelligent braking mechanisms which are easy to operate and also fuel efficient for applications such as the short loading cycle where the wheel loader driver has to perform repetitive operations in short times and tends to operate the machine as it is more convenient without regarding the fuel efficiency.

REFERENCES

- [1] B. Frank, L. Skogh, R. Filla, and A. Fröberg, "On increasing fuel efficiency by operator assistant systems in a wheel loader," *VTI 2012*, pp. 35–47, 2012.
- [2] V. Nezhadali, L. Eriksson, and A. Fröberg, "Optimal control of a wheel loader in the lift-transport section of the short loading cycle," *7th IFAC Symposium on Advances in Automotive Control*, AAC 2013.
- [3] Product brochure, Volvo L220G wheel loader "http://www.volvoce.com/constructionequipment/na/en-us/products/wheelloaders/wheelloaders/L220G/Pages/specifications.aspx", 2012.
- [4] PROPT, "http://www.tomdyn.com/", tomlab 7.9.
- [5] R. Filla, "Quantifying Operability of Working Machines," Ph.D. dissertation, Linköping University, Dissertation, NO. 1390, 2011.
- [6] J. Walström and L. Eriksson, "Modeling engines with a variable-geometry turbocharger and exhaust gas recirculation by optimization of model parameters for capturing non-linear system dynamics," *Proceedings of the Institution of Mechanical Engineers, Part D, Journal of Automobile Engineering*, vol. 225, pp. 960–986, 2011.
- [7] D. Hrovat and W. E. Tobler, "Bond graph modeling and computer simulation of automotive torque converters," *Journal of the Franklin Institute*, vol. 319, pp. 93–114, 1985.
- [8] L. Guzzella and A. Sciarretta, Eds., *Vehicle Propulsion Systems, Introduction to Modeling and Optimization*. Springer, 2007.